Geologie en Mijnbouw **76:** 247–266, 1997.

A Pan-African core complex in the Sinai, Egypt

B. Blasband, P. Brooijmans, P. Dirks*, W. Visser & S. White
Department of Geology, Institute of Earth Sciences, Utrecht University, P.O. Box 80021, 3508 TA Utrecht, the Netherlands; (present address: University of Zimbabwe, Mt. Pleasant, Harare, Zimbabwe)*

Received 12 November 1996; accepted in revised form 11 July 1997

Key words: extension, non-coaxial deformation, orogenic collapse, Precambrian

Abstract

In the late Precambrian history of the Wadi Kid area in the Sinai, Egypt, two deformation phases are clearly recognized. The first phase, D_1 (pre-620 Ma), produced a steep regional foliation, axial planar to upright F_1 folds, in rocks of a lower-greenschist grade. This compressional phase of deformation is interpreted in terms of subduction in an island-arc setting. The second phase, D_2 (post-620 Ma), is mainly expressed by the widespread development of sub-horizontal mylonitic zones with a total thickness of 1.5 km. Shear sense indicators give a consistent regional transport direction to the northwest, with local indications of reversal to the southeast. This event is associated with regional LP/HT metamorphism, indicative of high thermal gradients. Because of the LP/HT metamorphism, the change in geochemical nature of the granitoids, and the orientation of the dykes, we interpret the mylonitic zones as low-angle normal shear zones related to core-complex development during an extensional event with the transport reversal being induced by doming. We postulate that orogenic collapse was responsible for the transition from the D_1 compressional phase to the D_2 extensional phase.

Introduction

The nature of the Pan-African orogeny in the Arabo-Nubian Shield has been subject of debate over the last years. Many geologists believe that a compressional regime in an island-arc setting was responsible for the main tectonic features (e.g. Shackleton et al., 1980; Bentor, 1985; Vail, 1985; Ragab, 1993). However, in some recent studies large strike-slip zones are regarded as being the important tectonic feature; they are associated with extensional structures such as sedimentary basins and dykes (Stern, 1985; Husseini, 1988).

The Wadi Kid area in the Sinai, Egypt, was chosen as a key area to study the structural geology and tectonics of the Precambrian rocks of the Arabo-Nubian Shield. Just as two models exist for the overall evolution of this shield, there are also two different models for the evolution of the Precambrian in the Sinai. Shimron (1980, 1983) interprets the tectonic development in terms of a compressional island-arc setting with two deformation phases: a syn-sedimentary D_1 phase, responsible for the folding of the bedding (S_0), and a D_2 thrust-phase, mainly represented by the sub-horizontal foliation found throughout most of the Wadi Kid area. On the other hand, Reymer (1983, 1984) postulates that there was a D_1 compressional phase which took place in an island-arc setting similar to Shimron's D_1 phase, but he relates the D_2 structures to the diapiric emplacement of granites.

The aim of the present study is to investigate in particular the D_2 phase of deformation in the Wadi Kid area. Detailed field mapping, followed by a microstructural analysis of carefully selected samples, was undertaken. The combined results indicate that the sub-horizontal foliations, described by Shimron (1980, 1983) and Reymer (1983, 1984), are mylonitic in origin and related to extension. Consequently, we propose a radically different tectonic interpretation for the Wadi Kid area: that of a widespread core complex, resulting from orogenic collapse. The data supporting this conclusion are presented and discussed below, along with their implications for the tectonic evolution of the Wadi Kid area.

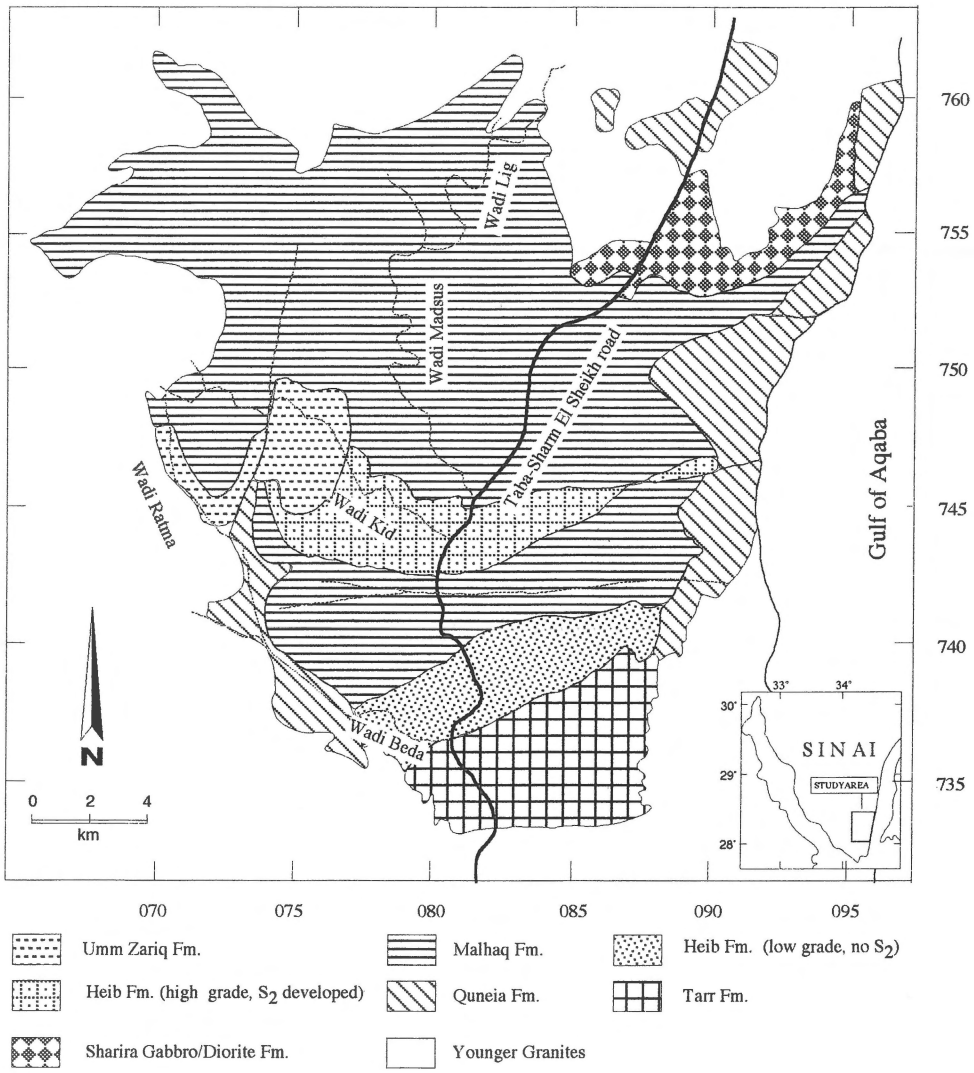

Figure 1. Generalized geological sketch map of the Wadi Kid area, modified after Shimron (1987).

Geological background

The Sinai peninsula consists at the surface mainly of sedimentary rocks (80%), ranging from Cambrian to Quaternary age, overlying the Precambrian crystalline basement. This basement forms a part of the Arabo-Nubian Shield, which extends over most of NE Africa and Arabia.

The recent geology of the Sinai is strongly influenced by the rifting of the Red Sea. Two orientations of faults are active since the Miocene: a NNE-SSW trend and a NW-SE trend. The metamorphic assemblages indicate that the total uplift did not exceed 15 km. The main phase of uplift took place during the Cambrian and was responsible for an uplift of at least 12 km. The post-Cretaceous tectonics are responsible for block rotation and another phase of uplift of 3 km (Kohn & Eyal 1981).

Lithology

The metamorphic and magmatic rocks making up the basement in the Wadi Kid area have been described by Shimron (1980, 1983, 1984), Furnes et al. (1985) and Reymer (1983, 1984). Their distribution is shown in Figure 1. The metamorphic and magmatic rock suites

are referred to as 'Formations' in the literature and we follow this terminology. The Umm Zariq Fm., Malhaq Fm., Heib Fm. and Tarr Fm. contain metasedimentary and metavolcanic rocks. The Quneia Fm. and the Sharira Gabbro/Diorite Fm. contain plutonic and meta-plutonic rocks. All these formations have been intruded by granites. The area is cross-cut by swarms of mafic and felsic dykes. The total thickness of the Precambrian metamorphic formations in the Sinai is at least 1.5 km.

The *Umm Zariq Fm.* is a metasedimentary sequence, mainly formed by metapelites; it contains also some metapsammites. The schistose metapelites contain biotite, muscovite, retrograde chlorite and feldspar along with porphyroblasts of garnet, andalusite and cordierite, indicating amphibolite facies of the low-pressure/high-temperature (LP/HT) type. Relict sedimentary structures, such as bedding, cross-bedding, slump structures and fining upward sequences, are found in the less schistose lenses. The rocks of the Umm Zariq Fm. are interpreted as metagreywackes.

The *Malhaq Fm.* is a metavolcanic sequence (Furnes et al., 1985) containing mainly schists and minor non-schistose massive equivalents. The schistose metavolcanics consist of feldspars, quartz, biotite and hornblende, indicating upper-amphibolite facies. The massive equivalents occur as layers and blocks within the schists and contain biotite, muscovite, chlorite, some quartz and feldspar.

The *Heib Fm.* is a mixed sequence of metasediments and metavolcanics. Rhyolitic and andesitic volcanics can be recognized. The metasedimentary sequence contains conglomerates and turbidites (the Beda Turbidites). The rocks display a lower metamorphic grade than the Umm Zariq and Malhaq Fms and are less deformed. In the more schistose parts, biotite and muscovite are observed, indicating a higher metamorphic grade. The lower-grade parts overlie the higher-grade parts of the Heib Fm. and of the Malhaq Fm. The rocks are thought to be of island-arc volcanic origin, deposited in a marine environment (Furnes et al., 1985).

The *Tarr Fm.*, found in the southern parts of the Wadi Kid, is dominantly a metasedimentary sequence consisting of metaconglomerates, metapelites and metapsammites, in which melanges and felsic flows can be recognized. The formation displays greenschist-grade metamorphism which is lower than that of the Malhaq and Umm Zariq Fms.

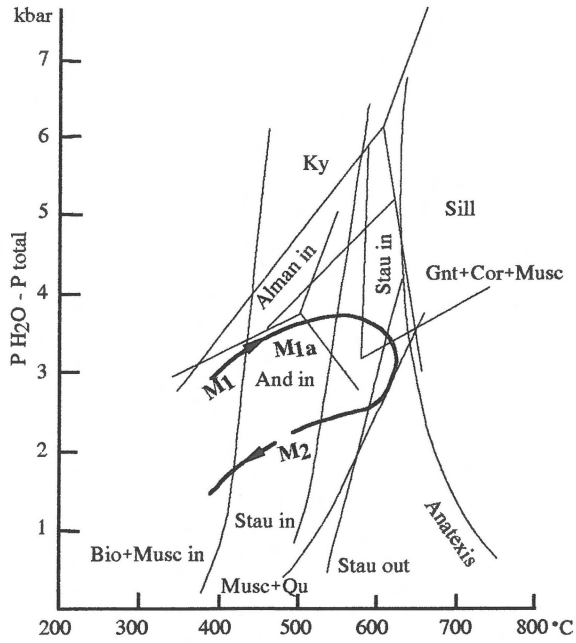

Figure 2. P-T-t path for alumino-silicate metamorphic rocks in the Wadi Kid area after Shimron (1987). The plot shows a clockwise path, starting with LP/LT (M_1) and moving to medium P and T. After upper greenschist facies was reached (M_{1a}), P remained constant at first and then started to go down but T continued to rise. Eventually, P and T both decreased during retrograde metamorphism related to uplift (M_2).

The *Quneia Fm.* consists of foliated and lineated diorites and tonalites with occasional biotite-rich xenoliths. Identical intrusives occur in the Nuweiba area, 100 km N of the Wadi Kid Complex, and these were interpreted, from geochemical data, as subduction-related I-type intrusives (Ahmed et al., 1993). Similar intrusives in the Timna area, 150 km N of the Wadi Kid area, were interpreted as I-type granitoids related to crustal thickening in an island-arc environment (Beyth et al., 1994).

Furnes et al. (1985) concluded on the basis of major and trace-element studies that the rocks of the metamorphic formations, described above, are subduction-related.

The *Sharira Gabbro/Diorite Fm.* occurs as a single large intrusive body in the northern part of the Wadi Kid Complex. It was described by Furnes et al. (1985) as a layered gabbroic and dioritic intrusion.

The Wadi Kid metamorphic complex is bordered to the north, west and south by *Younger Granites*. Three phases of granitoid intrusions were described (Bentor, 1984; Ahmed et al., 1993). The oldest plutonic rocks are the deformed tonalitic to granodioritic rocks of the

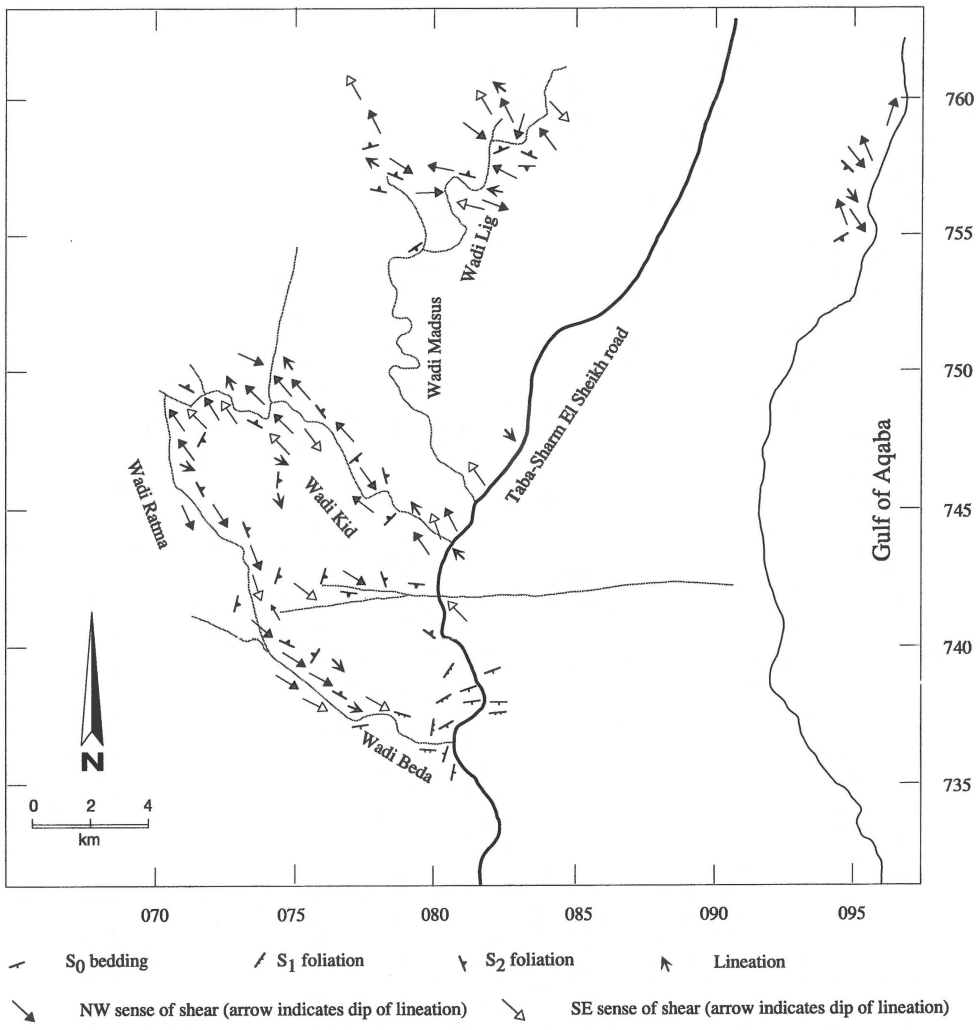

Figure 3. Map showing structures related to Precambrian tectonics in the Wadi Kid area.

Quneia Fm. The second phase consists of muscovite granites, which only occur in the most northern part of the Wadi Kid area. The youngest are the biotite-rich granites. Geochemical data indicate that the oldest granitoids are I-type, the muscovite-rich granites S-type, and the youngest biotite granites A-type granites (Ahmed et al., 1993). The S- and A-type intrusives are younger than any of the metamorphic rocks and mostly show intrusive contacts with these rocks. Trace-element studies of late Precambrian A-type granites in southern Israel indicate that these were formed in a thinned crust due to extension, where mantle melts were able to rise near to the surface (Beyth et al. 1994).

Metamorphism

Metamorphic grades of the Wadi Kid area range from lower-greenschist to amphibolite facies with a general trend of increase towards the central and northern parts of the area. Lower-greenschist-facies rocks dominate the southern areas. Sillimanite, garnet and andalusite porphyroblasts appear in the central Wadi Kid Complex where the metamorphic grade reaches upper-amphibolite facies. Here, staurolite is overgrown by andalusite and biotite, which indicates that a medium-pressure phase (> 5 kbar) preceded a LP/HT metamorphic phase. In the northern part of the area, where metavolcanic rocks are found, garnet and horn-

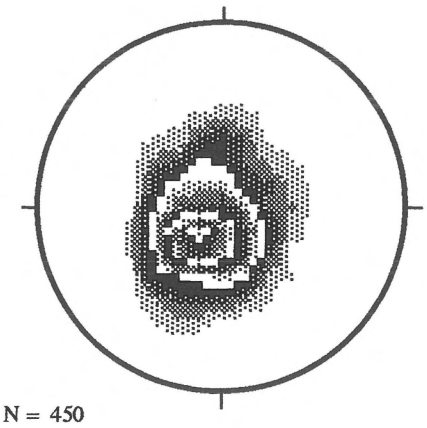

Figure 4. Contoured stereographic plot (equal area) of the poles to the S_2 foliation in the Wadi Kid area. Contour interval = 2.0%, significance level = 3.0.

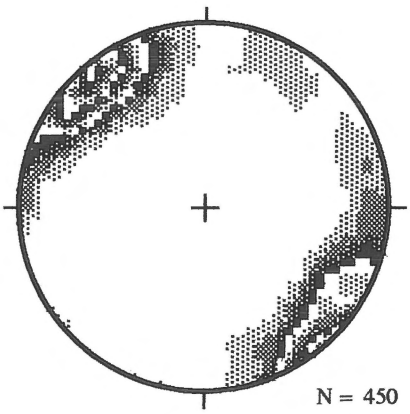

Figure 5. Contoured stereographic plot (equal area) of the lineations in the Wadi Kid area, showing maxima at NW and SE. Contour interval = 2.0%, significance level = 3.0.

blende porphyroblasts occur. In the north-eastern part, migmatites are present.

Reymer et al. (1984) calculated a temperature of 700 °C and a pressure of 3 to 4 kbar for the Malhaq and Umm Zariq Fms in the central Wadi Kid. Temperatures of 300 °C and pressures of 2 kbar have been deduced for the lower-greenschist-facies rocks in the southeastern part of the complex. The metamorphic grade in the Heib Fm. increases from lower greenschist in the Beda Turbidites in the southeast, to higher greenschist in the west and north where biotite-schists appear. Reymer et al. (1984) estimated that the thermal gradient was higher than 50 °C/km in the rocks showing amphibolite-grade metamorphism. Shimron (1987) constructed a clockwise P-T-t path for the metamorphic rocks in the Wadi Kid (Figure 2).

Geochronology

The limited number of isotopic ages available for the wider Wadi Kid area are summarized in Table 1. From these data it can be concluded that deposition of sediments and volcanics took place after 770 Ma and until 650 Ma ago (Priem et al., 1984), when the metamorphism started. The main amphibolite phase of metamorphism started at about 620 Ma ago. Pulses of metamorphism and the intrusion of granites continued till the early Cambrian and were accompanied by the intrusion of dykes (Ayalon et al., 1987).

The structural geology

The late Precambrian tectonic history of the Sinai has been divided by most authors (e.g. Shimron, 1980, 1983; Reymer, 1983, 1984) into two deformation phases, namely D_1 and D_2. The results of our structural study are presented in Figure 3. Our study focuses on the D_2 event because of its controversial nature in the tectonic models for the Sinai.

D_1 structures

The S_1 foliation is well developed in the lower-grade parts of the Heib Fm., such as the Beda Turbidites in the southern Wadi Kid area. The S_1 slaty cleavage, formed by white micas, is easily recognizable in the shaly layers within these meta-turbidites. It is oblique to the bedding. Inversion of the bedding can be recognized through bedding and cleavage relationships and through sedimentary structures such as cross bedding and coarsening upward sequences. Upright isoclinal F_1 folds are thus associated with the formation of the axial planar S_1 foliation. Shimron (1983) concluded that D_1 has taken place at shallow depth, soon after deposition. We agree with this, since the Heib Fm, was interpreted to have been deposited in an island-arc environment (Furnes et al., 1985), since these rocks display a low metamorphic grade where sedimentary structures are recognizable, and since accretion is the oldest tectonic process recognized in other parts of the Arabo-Nubian Shield (Bentor, 1985). The D_1 structures were thus formed in a compressional island-arc setting. F_1 folds and the associated cleavage are occasionally recog-

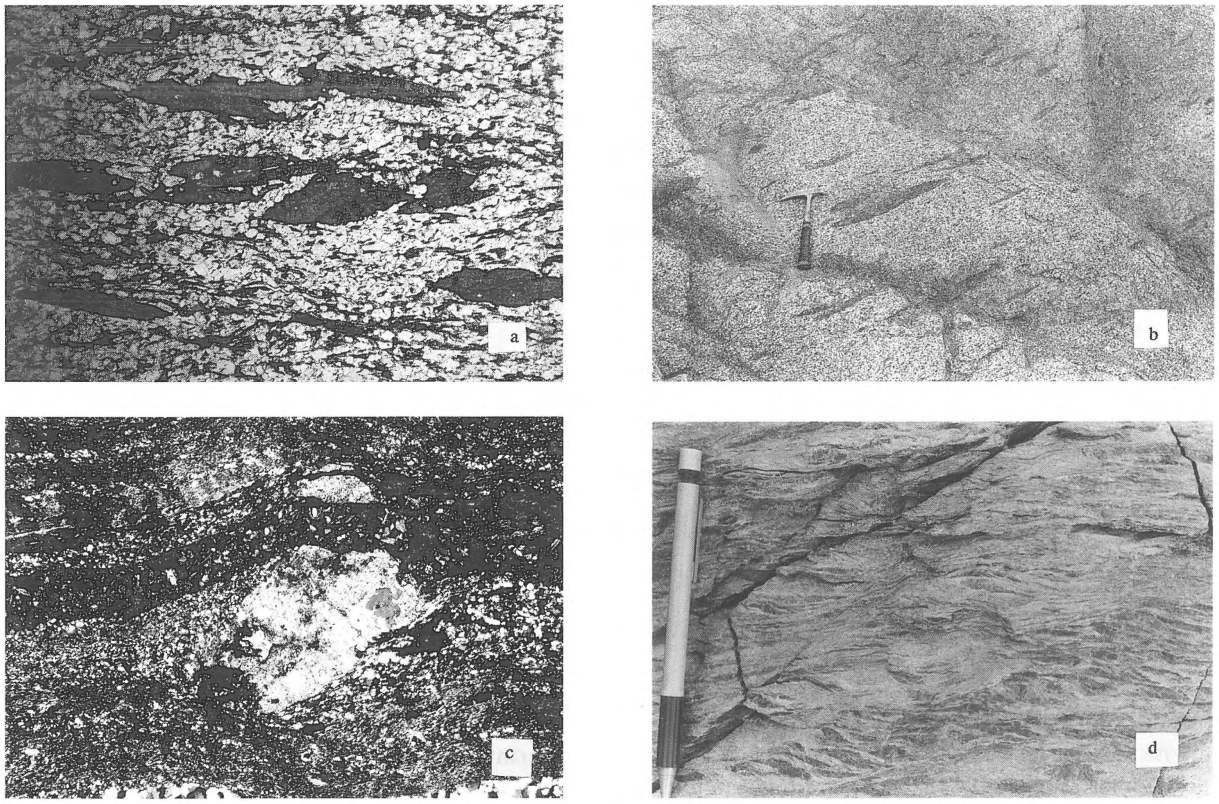

Figure 6. Photographs. a) Lineated hornblende, Malhaq Fm., northern Wadi Kid area. Area shown in 4.9 mm × 3.4 mm. b) Deformed xenoliths, Quneia Fm., NE part of the Wadi Kid area. c) Rotated clast with pressure shadows indicating sinistral sense of shear, Malhaq Fm., central Wadi Kid area. Area shown is 4.9 mm × 3.4 mm. d) Macroscopic extensional crenulation cleavage, indicating sinistral sense of shear, Umm Zariq Fm., central Wadi Kid area.

nized in the Umm Zariq Fm., with a steep foliation formed by muscovite and biotite. The D_1 structures in this formation were overprinted by a later foliation.

D_2 structures

S_2 foliation

The S_2 foliation is widely developed and dominates the studied area. It is flat-lying to gently dipping (< 30°, Figure 4) and in most areas it totally masks the earlier foliation. It is a disjunctive and sometimes anastomosing foliation, formed by biotite, muscovite and chlorite. The grains in the microlithons show a rather strong preferred orientation.

The general trend in the Wadi Kid Complex is that S_2 is better developed to the west and north. S_2 is best developed in the Malhaq, Umm Zariq and Quneia Fms. It is continuous through the higher-grade parts of the Heib Fm. into the Quneia Fm., indicating that the deformed tonalites and diorites of the Quneia Fm. were intruded before the development of S_2. Rocks containing D_1 structures overlie rocks displaying D_2 structures. Slightly foliated granites were observed in the western part of the Wadi Kid Complex. These intrusives were dated at 580–530 Ma as the youngest rocks of the Sinai basement (Bielski, 1982) and are thus critical for the timing of the deformation.

Lineations associated with S_2

A lineation is associated with the S_2 foliation and arises from an alignment of minerals such as andalusite and hornblende or from elliptical objects such as elongate xenoliths and pebbles. The lineation is sub-horizontal (< 30°), plunging either NW or SE (Figure 5), that is in opposite directions due to later folding. The two trends reflect one strain regime.

The mineral lineation is best developed on the S_2 plane in the schists. It is mainly defined by individual

Table 1. Summary of isotopic ages of Precambrian rocks in the wider Wadi Kid area. Bio, biotite; WR, whole rock; Zr, zircon.

Formation	Metamorphic grade	Age in Ma	Technique	Reference
Heib Fm. (rhyolitic flow)	–	770 ± 150	U-Pb (Zr)	H.N.A. Priem (unpubl. data)
Heib Fm. (granitic pebbles)	–	848 ± 61	U-Pb (Zr)	H.N.A. Priem (unpubl. data)
		735 ± 25	U-Pb (Zr)	H.N.A. Priem (unpubl. data)
Tarr Fm.	upper greenschist	616 ± 30	Rb-Sr (Wr)	Halpern & Tristan (1981)
Umm Zariq Fm.	amphibolite	609 ± 12	Rb-Sr (Wr)	Bielski (1982)
Malhaq Fm.	amphibolite	609 ± 12	Rb-Sr (Wr)	Bielski (1982)
Metavolcanic Ataqa schists	lower amphibolite	600 ± 10	Rb-Sr (Wr)	Ayalon et al. (1987)
(10 km N of Wadi Kid area)		566 – 529	K-Ar	Ayalon et al. (1987)
Def. diorite/tonalite	–	608 ± 7	Rb-Sr (Wr)	Siender et al. (1974)
Monzodiorite	–	625 ± 5	U-Pb (Zr)	Beyth et al. (1994)
(150 km N of Wadi Kid area)				
Dykes	–	591 ± 9	Rb-Sr (Wr)	Stern & Manton (1987)
Younger Granite	–	580 – 530	K-Ar (Bio)	Bielski (1982)

minerals that grew in one uniform direction: amphiboles, sillimanite, andalusite, quartz and feldspar. Some mineral lineations are formed by elongated pods of biotite, muscovite and by quartzo-feldspathic segregations. At some places the mica pods, andalusites, quartz and feldspars are mechaically elongated and define a stretching lineation (Figure 6a). It is concluded that the lineation was formed partly by stretching, partly by orientated growth. The stretching lineation indicates an extensional strain in NW-SE direction; this will be discussed later. In a number of cases the elongated minerals, mainly andalusites and hornblendes, grew in random directions; this was observed in the Umm Zariq and Malhaq Fms. Their significance will likewise be discussed later.

Elongated pebbles were found in the conglomerates of the high-grade parts of the Heib Fm., and elongated xenoliths in the deformed intrusives of the Quneia Fm. They are parallel to the general trend of the mineral lineation.

Dykes

The area is cross-cut by vertical felsic and mafic dyke swarms of Precambrian age. They are sub-parallel and strike 35 to 50°, i.e. NE-SW (Figure 7). Both types of dykes intruded at 590–580 Ma (Halpern, 1980; Stern & Manton, 1987). This age is close to the D_2 ages. Along with their orientation, the contemporaneity suggests that the intrusion was related to the D_2 phase.

Dyke swarms require lateral extension in the crust and the intrusion plane will be perpendicular to σ_3, the direction of greatest extension (Price & Cosgrove, 1990). The dykes thus indicate extension in the NW-SE direction at the time of D_2, the same direction as can be deduced from the stretching lineation.

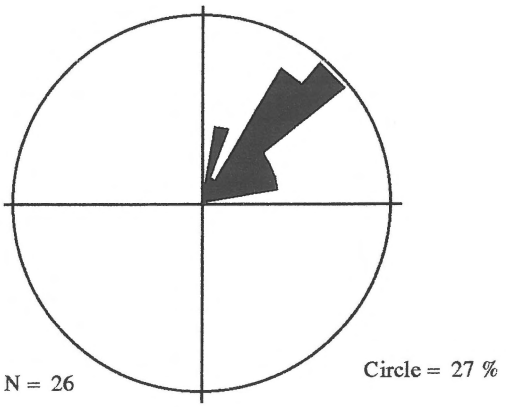

Figure 7. Rose diagram of the orientation of the mafic and felsic dykes in the Wadi Kid area.

Evidence of non-coaxial strains during D_2

Previously, D_2-structures have been interpreted as due to an irrotational and a coaxial strain regime (e.g. Reymer, 1983, 1984; Shimron, 1983, 1984). However, in the course of this study we consistently found that rotational strains were present. Several possible indicators of non-coaxial strain were observed: extensional crenulation cleavage, S-C shearbands, rotated clasts with pressure shadows, asymmetric folds, deformed elliptical objects and quartz c-axis fabrics. The impor-

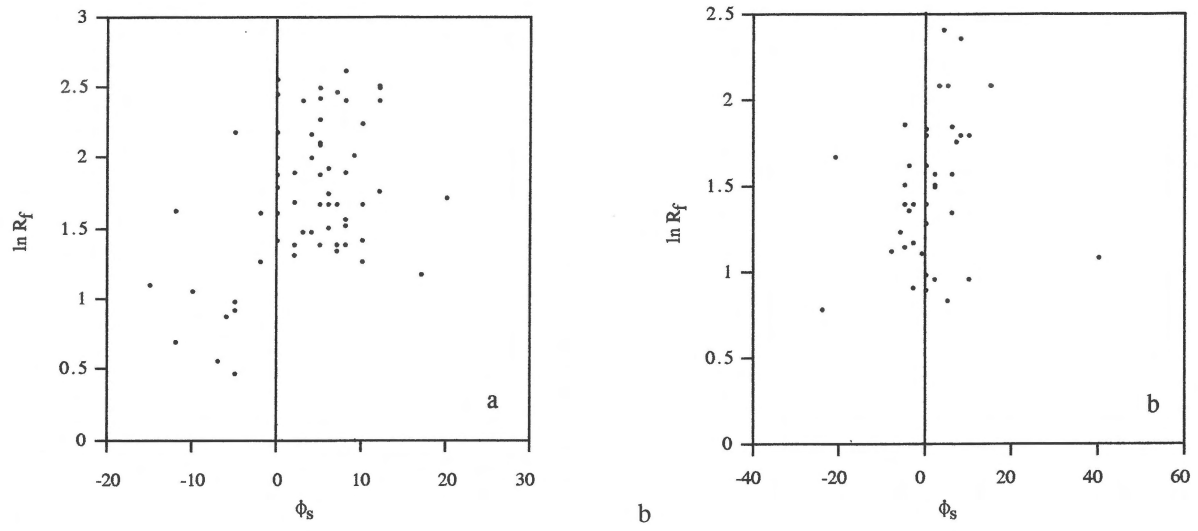

Figure 8. R_f/Φ plots of deformed xenoliths, Quneia Fm., NE part of Wadi Kid area. a) The X-Z section reveals the asymmetry with respect to $\Phi = 0$ and the internal asymmetry. b) In the Y-Z section no asymmetry is visible.

tance and reliability of these indicators will be discussed below.

Figure 3 shows the distribution of shear indicators with the sense of shear and the recorded stretching and mineral lineations. The strain was evaluated for elliptical markers.

Finite strain markers

Throughout the Wadi Kid area, elliptical markers, namely xenoliths, conglomerate pebbles and boudins, were found. They can be used for a qualitative and quantitative strain analysis. These markers are regarded as good indicators of the total finite strain (Lisle, 1985), which is very useful in areas with a complicated strain history. Different methods were developed to determine the strain of deformed elliptical objects, taking into account that the initial shape was not spherical and that the markers had a non-random initial orientation.

The tests for non-coaxiality were performed on deformed xenoliths, conglomerate pebbles and boudins. The xenoliths were used to perform a strain analysis with the R_f/Φ method (Dunnet, 1969; Lisle, 1985). The deformed conglomerate pebbles and boudins were used for qualitative analysis and in this framework their relationships with other structural features were studied.

In the northeastern part of the Wadi Kid area, elliptical mafic xenoliths were found in a foliated and lineated syn-kinematic diorite which intruded during D_2 (Figure 6b). The foliation in the schistose xenoliths continues into the diorite. The stretching lineation of hornblendes in the diorite is sub-parallel with the longest axes of the xenoliths.

The basic method, used to compute the strain, is that of Ramsay-Dunnet modified by Lisle (1985) for elliptical markers with an initial ellipticity (R_i). This is a graphical method to compute the ellipticity of the strain ellipse (R_s) from R_f (the final ellipticity) and the angle between the long axis of the elliptical marker and the orientation plane, in the deformed state, Φ_s. The results of the R_f/Φ method were compared to the harmonic mean, H, which gives a good approximation of R_S (Lisle, 1977).

The xenoliths in the Wadi Kid area have an elliptical form and show a uniform direction of their principal axes, with the longest axis (X-axis) sub-parallel with the mineral lineation. The Z-axis is the axis of greatest shortening, so that X > Y > Z. The foliation was chosen as the reference plane. The X : Z ratio was measured on a plane parallel with the lineation and perpendicular to the foliation. Φ_s is the angle between the X-axis and the foliation in the case of the X-Z section, and that between the Y-axis and the foliation in the case of the Y-Z section. Φ_s was chosen positive when the orientation of the X-axis was dipping steeper to the southeast than

the reference plane. The Y : Z ratio was measured on a plane perpendicular to the lineation and perpendicular to the foliation.

Eighty-five measurements were made on the X-Z plane. The final ellipticity, R_f, for X-Z ranges from 1.58 to 13.5. Figure 8a shows the R_f/Φ plot for X-Z. The plot shows an asymmetric distribution of points around the mean vector $\Phi = 3.41°$. From the R_f/Φ diagram, values for $R_S = 4.6$ and $R_i = 2–2.5$ are deduced. The harmonic mean, H, is 4.71. From H and the R_f/Φ plot it can be concluded that $R_S = 4.6–4.7$. The mean vector, Φ, is 3.41° and so the distribution of points is asymmetric with respect to $\Phi = 0$. The longest axis of the plot is not parallel to the vertical base axis, revealing an internal asymmetry.

Forty measurements were made on the Y-Z plane. The R_f for Y-Z ranges from 2.167 to 11. Figure 8b shows the R_f/Φ diagram for Y-Z. The distribution of the points is symmetrical around the $\Phi = 0$ axis. From the diagram, values for $R_S = 4.2$ and $R_i = 1.5–2.0$ are deduced. The harmonic mean, H, gives a value of 3.95. Since H is expected to give lower values than R_S (Lisle, 1977), 3.95 should be a good indication for the maximum of R_S in the Y-Z plane.

Other deformed elliptical objects, such as elongated conglomerate pebbles and asymmetric elongated boudins, occur throughout the Wadi Kid area. The former were found in the relatively high-grade parts of the Heib Fm. in the central Wadi Kid area and the latter where S_2 was developed. These elliptical objects have their longest axis sub-parallel with the mineral lineation and plunge slightly steeper to the southeast than the foliation, thus showing the same structural relationships with the lineation and the foliation as the xenoliths. The deformed conglomerates and boudins show, like the deformed xenoliths, a movement of the top block to the northwest. The identical morphology and structural relations of all the deformed elliptical markers indicate a similar deformation history for all the total finite strain markers.

Conclusions on finite strain markers. The R_f/Φ method is a suitable method to analyse the strain of the xenoliths, but additional data from statistic and geometrical methods are required to obtain a precise indication of the amount of strain and the initial form. Lisle (1985) showed that H gives a good approximation for R_S and used this method in cases of asymmetric distribution in R_f/Φ plots. Best values for the X : Y : Z relationship were calculated to be 4.6 : 3.95 : 1. From this relationship it is clear that a large component of flattening is present.

The mean vector of the X-Z plane is 3.41° and thus asymmetric with respect to $\Phi = 0$. The R_f/Φ plot for this plane also shows an internal asymmetric distribution. The mean vector Φ for the Y-Z plane is close to 0° and the R_f/Φ plot shows a symmetric distribution, and thus no asymmetry with respect to the reference plane exists. Internal asymmetries in R_f/Φ plots are ascribed to a preferred initial orientation of the elliptical objects (Lisle, 1985), which can be explained by the fact that xenoliths in syn-kinematic intrusions will have a preferred initial orientation. The asymmetry with respect to $\Phi = 0$ is best explained as due to non-coaxial deformation (Le Theoff 1979, Choukroune et al. 1987). The X-axis is parallel to the stretching lineation but plunges steeper to the southeast than the foliation and lineation, and thus the finite strain markers indicate a NW-vergent movement of the top block during a regional shear event.

The deformed pebbles, xenoliths and boudins show the same relationships with other structural features: lineation and foliation. Since they were deposited or initially formed under different conditions, their final stage of deformation must have been similar. The asymmetry is found in the X-Z plane, parallel with the lineation and the movement direction. No asymmetry was observed in the Y-Z direction. This indicates non-coaxial deformation with the axis of rotation perpendicular to the X-Z section and movement of the top block to the northwest.

Kinematic indicators

Rotated clasts

Rotated clasts with asymmetric pressure shadows were observed in a number of thin sections from the Wadi Kid area (Figure 6c). They are regarded as good indicators of the sense of displacement (Simpson & Schmid, 1983) if applied as indicated by Ten Brink (1996). The rotated pressure shadows are of the displacement-controlled type with deformable fibers. These fibers indicate relatively high temperatures, allowing dynamic recrystallization. Table 3 and Figure 3 show that shear took place in two opposite directions, with the top-to-the-NW direction dominating. Some clasts are accompanied by symmetric pressure shadows. This can indicate a component of coaxial deformation, or a reversal of the shear direction, re-deforming the fibers.

Table 2. Results of quartz c-axis study of samples from the Wadi Kid area. For locations see Figure 9.

Sample	Rock type	Metamorphic grade	Fabric group (see text)	Likely slip system	Movement deduced from quartz c-axis fabrics	Movement deduced from other features	Comments
B 18	hbl-bio schist	amphibolite	3	basal <a> and ± rhomb <c + a>	NW	NW (e.c.c. and rotated clasts)	A component of flattening
B 20	hbl-bio schist	amphibolite	2	prism <a> with basal <a>	SE	NW (e.c.c.)	–
B 29	hbl-bio schist	upper greenschist – lower amphibolite	2	prism <a> with basal <a> and rhomb <a>	SE	SE (rotated clasts)	A component of flattening
P 61	hbl-bio schist	upper amphibolite	3	basal <a> and ± rhomb <c + a>	NW	NW (e.c.c.)	A small component of flattening
P 16	and-gnt-bio schist	amphibolite	3	basal <a> and ± rhomb <c + a>	SE	NW (e.c.c.)	Outcrops in this area show SE shear
P 17	sill-gnt-bio schist	amphibolite	3	prism <a> with basal <a>	SE	SE (e.c.c.)	A component of flattening
P 37	deformed tonalite	–	2	prism <a> with basal <a>	NW	NW (deformed xenoliths)	A small component of flattening
P 39	deformed tonalite	–	3	prism <a> and ± <c + a>	NW	–	A component of flattening
WJ 9	and-gnt-bio gneiss	amphibolite	1	basal <a> and minor prism and rhomb <a>	NW	NW (e.c.c.)	–
WJ 22	deformed granite	–	1	basal <a> with significant rhomb <a>	NW	–	Deformed younger granite
WJ 29	bio schist	greenschist	2	prism <a> with basal <a>	NW	NW (e.c.c.)	A component of flattening
WJ 42	bio schist	greenschist	1	basal <a>	SE	NW (rotated clasts)	–

Extensional crenulation cleavages

Throughout the area, extensional crenulation cleavages (e.c.c.) were observed. They develop in the late stages of shear zone activity (Platt & Vissers, 1980) and are regarded as a good indication of local shear movement.

The e.c.c.'s in the Wadi Kid are found both on meso-scale (Figure 6d) and on micro-scale. They contain biotites, white micas, hornblendes and andalusites, depending on the metamorphic assemblage in the country rock. Table 3 and Figure 3 show that the e.c.c.'s, like the rotated clasts, display top-to-the-NW as well as a top-to-the-SE shear, with the NW transport dominating. Hornblende occurs mostly in the e.c.c.'s with a sense of shear to the northwest. White mica appears in e.c.c.'s with a NW sense of shear as well as in e.c.c.'s with a SE sense of shear, but is relatively abundant in the latter e.c.c.'s. We relate the formation of the white mica with a phase of retrograde metamorphism and so the SE sense of shear postdated the NW sense of shear.

Asymmetric folds

Although asymmetric folds can be used as shear indicators, they are not very reliable (Bell & Hammond 1984). Their reliability improves when they are viewed perpendicular to the stretching lineation, as was done in this study. During progressive deformation, fold axes tend to rotate parallel to the movement direction and are thus of little value in determining the sense of movement. The few asymmetric folds that were found in the Wadi Kid area indicate a NW sense of shear.

Quartz c-axes as indicators for non-coaxial deformation

Quartz fabrics record deformation caused by plastic deformation mechanisms and can give information

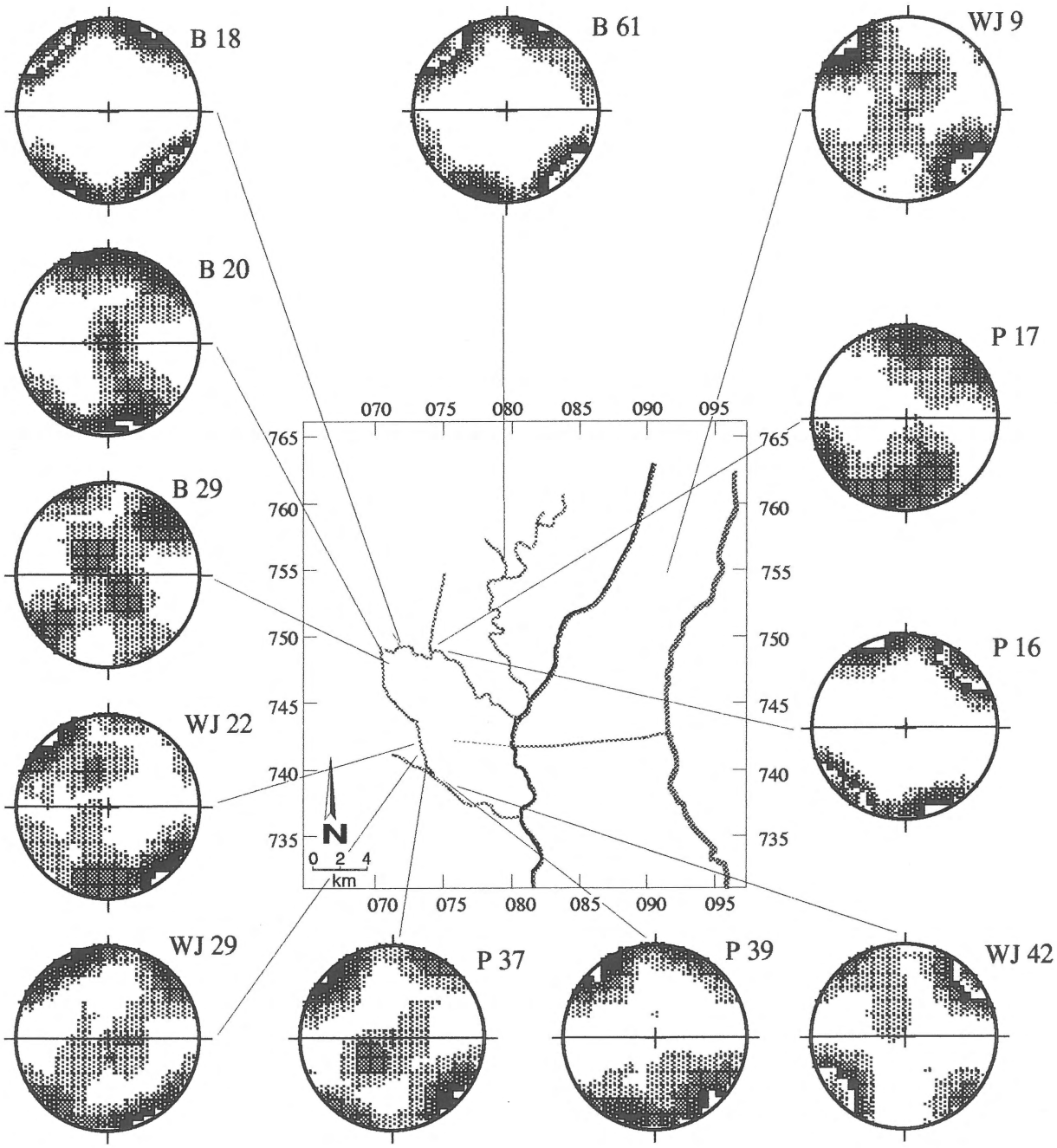

Figure 9. Locations and quartz c-axis fabrics of the studied samples listed in Table 2. Contour interval = 2.0%, significance level = 3.0.

about the type and conditions of deformation (Price, 1985). Coaxial deformation produces symmetrical patterns with respect to the principal axes of finite strain and thus with respect to the foliation, whereas non-coaxial deformation produces an asymmetric fabric. The latter points to a mylonitic origin of a schistose rock. The type of slip system in the quartz grains can be deduced from the quartz c-axis fabric, thus providing an indication of the relative temperature at which the deformation took place.

The samples used in the quartz c-axis studies were cut parallel to the lineation and perpendicular to the

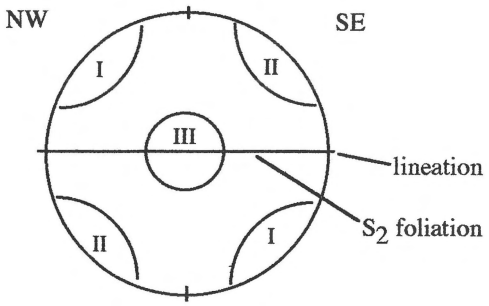

Figure 10. Positions of the different maxima in the quartz c-axis plot.

foliation. Twelve samples were chosen from the Wadi Kid Complex. A minimum of 125 grain measurements were made on each sample. Figure 9 shows the location and quartz fabrics of the studied samples. Figure 10 shows the position of the different maxima in a quartz c-axis plot (after Fueten et al. 1991); this plot was used for the interpretation of the fabrics. Table 2 summarizes the results of the quartz c-axis studies. On the basis of their patterns, the quartz c-axis fabrics were divided into three groups. These groups indicate different slip systems and consequently different conditions of deformation.

Samples WJ 9, WJ 22 and WJ 42 belong to the *first group*. Their fabrics display single girdles and maxima are best developed at I or II. The maxima are at angles of 30° with the lineation. This fabric indicates slip along the basal plane in the <a> direction plus minor activity on the rhomb and prism in an <a> direction and is indicative of relatively low temperatures of deformation (Jessel & Lister 1990).

WJ 42 comes from the transitional area between low-grade and high-grade Heib Fm. and formed at relatively low temperature. The fabric asymmetry indicates top-to-the-NW movement. Rotated clasts in this sample show a reverse shear direction. Quartz c-axis fabrics will, in most cases, record the last stages of deformation (Lister & Hobbs 1980) and it is also likely that the last increments of deformation will be concentrated in the quartz-rich bands. The rotated clasts are thus indicative of the earlier stages of deformation and the quartz fabric of WJ 42 is reflecting a later overprint. Sample WJ 9 shows the same characteristics of deformation as WJ 42, but the mineralogy of this rock indicates a higher metamorphic grade. The fabric shows movement of the top block to the northwest indicating deformation after peak metamorphism.

Sample WJ 22 did not show any macroscopic or microscopic shear indicators, but a clear quartz fabric asymmetry was observed, indicating movement of the top block to the northwest. The c-axis fabric indicates basal <a> slip with a significant rhombic component, which takes place at low to medium temperatures. From WJ 22 it can be concluded that deformation continued to take place until the later stages of cooling and thus relatively late in the development of the Sinai basement.

The *second group* of quartz c-axis fabrics is distinguished from other groups by the fact that the fabrics contain a maximum at III. This maximum is connected with the maxima and I and/or II via a girdle, depending on the shear-direction. The maximum at III indicates that the prism <a> slip system was active, which indicates that deformation took place at medium temperatures (Tullis et al. 1973, Schmidt & Casey 1986). The basal <a> and prism <a> slip systems are thus active in this group.

Samples B 20, B 29, P 37 and WJ 29 belong to this group. In sample B 29, c-axes appear between III and I, indicating that also the rhomb <a> slip system was active and that deformation took place at intermediate-high temperatures. This sample indicates a movement of the top block to the southeast. Sample WJ 29 is a biotite schist from the high-grade part of the Heib Fm. near the contact with granitoid rocks. It displays a NW-vergent sense of shear. Sample B 20 is from the relatively high-grade rocks of the Malhaq Fm. and indicates a top-to-the-SE movement. Sample P 37 comes from the slightly foliated tonalites in the Wadi Quneia/Wadi Ratma area and displays a movement of the top-block to the northwest. It shows less evidence for rhomb slip, as the prism and basal sections are more isolated.

The samples of the *third group* have strong maxima at I and at II, but in all cases one of the two maxima was better developed than the other and no maxima are found in III. The angles between the I and II maxima are 50°. They resemble small-circle girdle fabrics and are a special case of type-I crossed girdles (Schmidt & Casey 1986). This fabric shows strong flattening. The active slip systems were basal <a> with rhomb <c+a>, indicative of deformation at medium to higher temperatures.

Samples B 18, B 61, P 16 and P 39 belong to this third group. Samples B 18 and B 61 are from the high-grade biotite schists of the Malhaq Fm. Both show a NW sense of shear with a rather strong flattening. Sample P 16 is from the high-grade metapelites of the Umm Zariq Fm. The fabric indicates movement to the

southeast but other shear indicators in this sample show a NW movement. At other outcrops in this area SE-vergent shear indicators were observed. Sample P 39 is from the gneissic tonalites of the Quneia Fm., and displays a NW sense of shear.

All studied samples show a well-developed quartz c-axis fabric. The individual fabrics display an asymmetry, indicating non-coaxial deformation. The three groups were distinguished on the basis of the fabric, which is related to the temperature of deformation. Deformation temperatures vary from relatively low to intermediate-high metamorphic conditions. The single-girdle fabrics (group 1) come from the lower-grade rocks, which are found at the upper structural levels. Higher-grade rocks (groups 2 and 3) were deformed at higher temperatures and are from a structurally lower level throughout the complex. These high-grade samples show a more coaxial type of deformation. Movement reversals appear also in the quartz c-axis fabrics and will be discussed later.

Sample WJ 22 shows non-coaxial deformation in a relatively late granite (530 Ma, Bielski 1982) implying that the deformation continued after the intrusion of this body.

Discussion

Interpretation of regional structural data

Our study indicates that in the Wadi Kid area a clear distinction can be made between D_1 and D_2 structures on the basis of the types of structures and their metamorphic grades. The D_1 structures consist of an axial planar slaty cleavage, namely S_1 foliations related to F_1 isoclinal folds. The F_1 folds in lower-grade rocks were formed in a compressional regime. No indicators of non-coaxial deformation were observed in these relatively low-grade rocks.

The second deformation phase, D_2, formed a flat-lying foliation (S_2) which is the most important structure in the area. The abundant evidence of asymmetry indicates that the areas of intense foliation-development mark D_2 shear zones.

The elongated minerals, formed on S_2 surfaces, are mostly orientated in NW-SE direction. Stretching of the elongated minerals indicates that peak-metamorphism started before or during D_2. The growth in a preferred parallel orientation of hornblende, andalusite and sillimanite indicates that peak-metamorphism continued during D_2. Randomly orientated hornblendes and andalusites were also found and could indicate either that peak-metamorphism outlasted D_2 or that the randomly orientated minerals grew in low-strain pockets, implying that the strain regime was not active through the whole shear zone during the entire deformation phase. The latter interpretation seems to fit best the observations in the Wadi Kid area.

The Wadi Kid area is cross-cut by dykes in NE-SW direction, perpendicular to the NW-SE trending lineation. This indicates that extension took place in NW-SE direction.

The indicators of non-coaxial strain were only found in the areas where S_2 was developed. Table 3 summarizes the different types of shear indicators with the sense of movement. Deformed pebbles, boudins and xenoliths are indicators of total finite strain and all show a non-coaxial deformation with movement of the top block to the northwest. Other non-coaxial shear indicators, such as rotated clasts with pressure shadows, extensional crenulation cleavages and quartz c-axis fabrics, predominantly produce a NW sense of shear but some indicate the reverse direction. From the structural map (Figure 3) it is difficult to indicate certain areas with one sense of shear and other areas with the reverse sense, but it was rare that within one outcrop (i.e. on a metre scale) shear indicators with opposite sense were found. The distribution of the sense of shear is thus heterogeneous.

The duality in shear sense may be ascribed to coaxial deformation when flexural slip took place in different limbs of a fold. However, this does not agree with the trend of the S_2 foliation and the direction of extension, nor with many of the asymmetric features. Because these latter features are abundant and form synthetically a well-developed stretching lineation, the foliation can be interpreted as a mylonitic foliation resulting from flat-lying shear zones. The main movement of the top block in the Wadi Kid area was interpreted to be to the northwest, since finite strain markers and some 70% of the shear indicators were found to indicate a NW sense of shear.

A core-complex model for the Wadi Kid area

A cross section of the Wadi Kid area according to our interpretation is shown in Figure 11. The relationship between the sub-horizontal mylonitic sequences formed in an extensional regime, the upper-crustal low-grade rocks related to an early compressive tectonic phase, the high metamorphic gradients, and the syn-tectonic granitoids as observed in the area, indicate

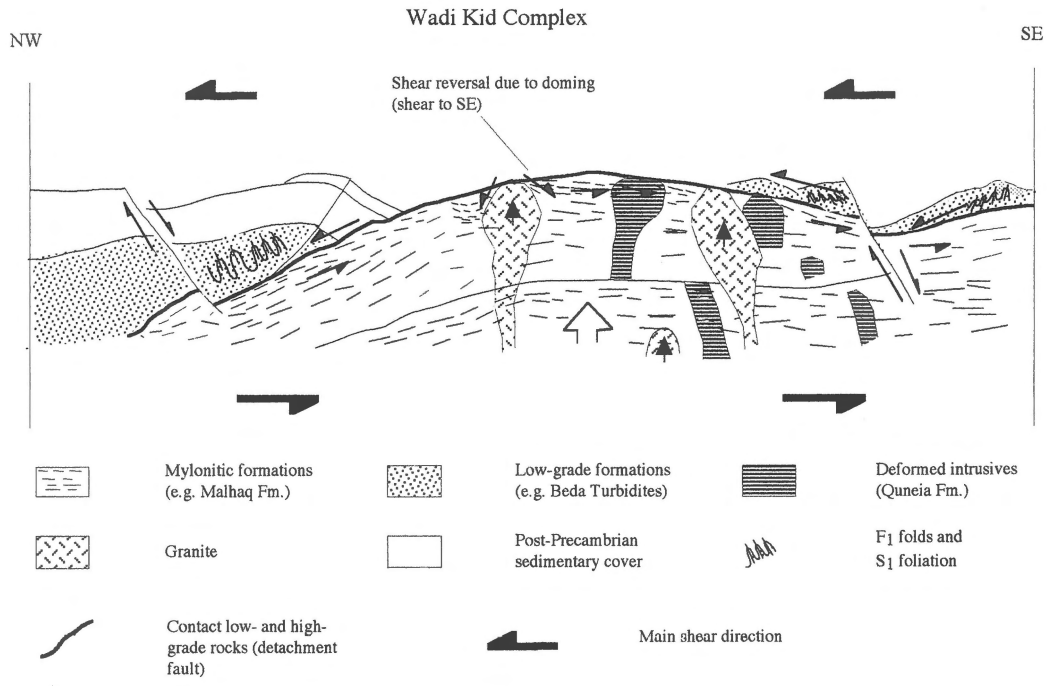

Figure 11. Schematic interpreted cross-section through the Wadi Kid Complex. High-angle normal faults were formed during the opening of the Gulf of Aqaba in the Miocene. The sedimentary cover is found to the northwest of the Wadi Kid area mapped in Figure 1. Length of section is approximately 50 km, height is approximately 10 km.

Table 3. The numbers and senses of movement of the different shear indicators, observed in the Wadi Kid area. The majority of them indicate a NW-vergent sense of shear.

Type of shear sense indicator	Macro.		Micro.	
	NW	SE	NW	SE
Deformed elliptical objects	10	–	–	–
Rotated clasts	5	4	12	5
Extensional crenulation cleavage	20	11	21	8
S-C fabrics	1	–	1	–
Asymmetric folds	6	1	–	–
Quartz c-axis fabrics	–	–	7	5

together a core-complex development. This is investigated below. Much has been published about core complexes in a variety of localities such as the Basin and Range province, U.S.A. (Davis 1980, Davis & Lister 1988), the Canadian Cordillera (Malavieille, 1987; Liu & Furlong, 1993), the Aegean Sea, Greece (Lister et al., 1984), and Variscan core complexes in the Massif Central, France (Malavieille 1993). Below, some of the most important characteristics found in these core complexes are reviewed and compared to those of the Wadi Kid Complex.

The ideal core complex consists of a core of granitoids, gneisses and other lower crustal rocks, overlain by a major mylonite zone. Relatively low-grade rocks, preserving relicts of an earlier deformation phase, overlie this zone. The mylonite zone tends to be subhorizontal with a near-constant direction of the stretching lineation through the whole area (Davis, 1980). The mylonites form at depths of at least 10 km and at temperatures of at least 500 °C, with a thermal gradient of $\geq$ 50°/km, and at pressures of 3.5 to 4.5 kbar (Davis & Lister 1988). The mylonitic zones normally have a thickness of about 1 km but may reach a thickness of 3.5 km (Davis & Lister 1988). The mylonitic rocks are generally interpreted as gently dipping low-angle normal shear zones of the type envisaged by Wernicke (1985), and are related to continental extension. The mylonites contain indicators of non-coaxial deformation which show the general direction of movement. However, in many cases a mixed mode of deformation, i.e. non-coaxial and coaxial deformation, is found and reversal of the sense of shear is observed (Malavieille 1993). The complicated deformation history makes kinematic interpretation difficult but this is characteristic of strain development in an extensional core-complex setting (Malavieille 1993). Undeformed

younger intrusives cross-cut all other sequences of the complex.

The core in the Wadi Kid metamorphic complex consists of deformed tonalites and diorites of the Quneia Fm., which have a gneissic appearance. Gneissic rocks were also described in other parts of the Sinai (Shimron 1980, Stern & Manton 1987). The mylonitic Malhaq and Umm Zariq Fms and the northern and western high-grade parts of the Heib Fm. form the mylonitic drape over the core. This drape is approximately 1.5 km thick. These formations contain a subhorizontal foliation with a constant NW-SE trending stretching lineation. The low-grade rocks of the Heib Fm., overlying the mylonitic formations, form the upper part of the core complex, with the D_1 compressive phase as a relict of an earlier deformation event. Metamorphism in the mylonitic formations is of a LP/HT type (Shimron 1987). The thermal gradient was $\geq 50°$/km and the foliated formations were formed at a depth of at least 10 km (Reymer et al. 1984).

In the Wadi Kid area a large variety and large number of shear sense indicators were observed. The axis of rotation of the sense of asymmetry from the kinematic indicators is always perpendicular to the stretching lineation. About 70% of the shear sense indicators show movement of the top block to the northwest; the rest shows movement to the southeast (Table 3). Part of the non-coaxial strain markers show a coaxial component. All the finite strain markers, indicators of the total strain, point to a sense of shear to the northwest. For this reason the mylonitic formations are interpreted as low-angle shear zones with a movement of the top block to the northwest.

The formation of core complexes is accompanied by extensive magmatism. Basaltic intrusives and syn-kinematic dykes intruded perpendicular to the direction of extension (Anderson & Cullers 1990, Hazlett 1990). Diorites and granodiorites, often syn-kinematic, are the oldest intrusives in core complexes (Barton 1990, Anderson & Cullers 1990). Younger granitoids, intruded during the extensional phase, have a more alkaline granitoid composition (Barton 1990, Anderson & Cullers 1990). In the Wadi Kid area the dykes strike NE-SW, perpendicular to the lineation and thus indicating extension in the NW-SE direction during D_2. The older intrusives are I-type granitoids, and younger intrusives are A-type alkaline granites (Ahmed et al., 1993). In other parts of the Arabo-Nubian Shield the older I-type granites are interpreted to have been related to a phase of crustal thickening during orogenic compression, while the A-type granites are interpreted to have been related to extension and crustal thinning when melts were arising from the mantle (Beyth et al. 1994, Greiling et al. 1994).

The features observed in core complexes such as that in the Wadi Kid area, are best explained as developing during orogenic collapse (Dewey 1988). The orogenic history starts with a period of compression and crustal thickening. When convergence slows down, thermal re-equilibration will start. Erosion and convective thinning of the root will cause extension and associated with this, there will be an increase in magmatic activity. The thermal gradient will increase rapidly. The extension may be accommodated by low-angle shear zones (Wernicke 1985). The metamorphism will show a clockwise P-T-t path, characterizing uplift in an extensional setting after a compressional phase, as is the case in the Wadi Kid area.

Reversal in the sense of shear and coaxial overprint in core complexes

The presence of opposing senses of shear and of components of coaxial deformation posed problems in the kinematic interpretation of the Wadi Kid area, where some 70% of the shear indicators show a top-to-the-NW movement and the rest shows movement to the southeast. Since all finite strain markers show the top-to-the-NW movement, the main deformational event is interpreted to have this sense of shear. Reversal of shear sense and minor components of coaxial deformation are regarded as characteristic features of core complexes (Malavieille 1987, 1993, Davis & Lister 1988, Spencer 1984, Reynolds & Lister 1990, Gautier & Brun 1994). Reynolds & Lister (1990), Malavieille (1993) and Gautier & Brun (1994) suggested that upward bending of the lower plate as an isostatic response to tectonic denudation and doming above plutons can cause shear reversal. In such cases the shear zone will undergo uplift and flexure, and parts of the shear zone will eventually dip to the opposite direction. Movement in the initial direction will stop in these parts of the shear zone, and reverse movement will start. The reverse sense of shear is thus a later overprint feature.

Gravimetric and aeromagnetic studies indicate the presence of elongate NE-SW trending intrusive bodies in the Sinai (Folkman & Assael 1980a, b, Ghazala 1995). The reversal of shear sense took place in the later stages of the development of the Wadi Kid area and is thus related to the intrusion of the younger NE-SW trending granitic plutons near this area, when uplift

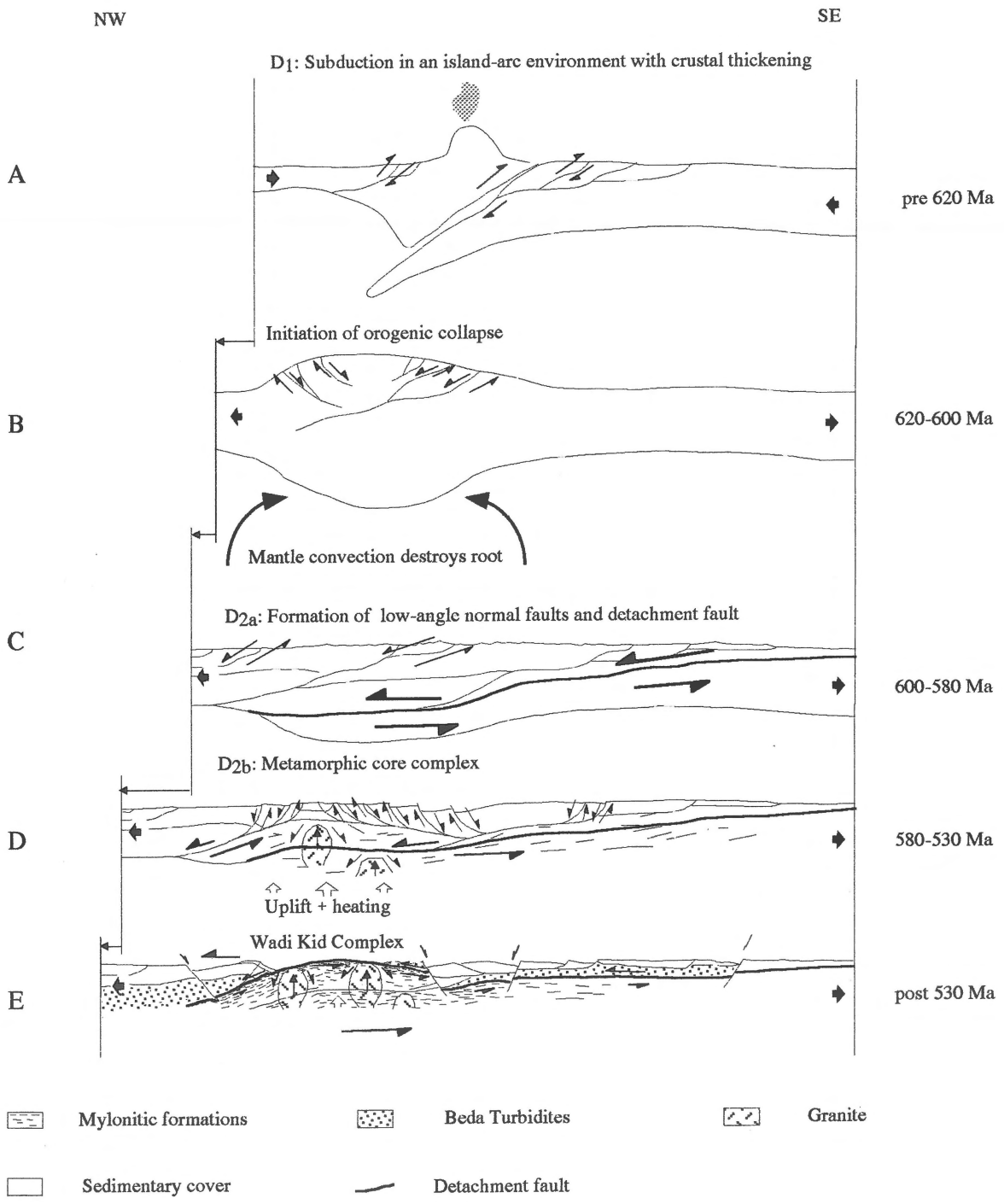

Figure 12. Model for the different stages of the formation of the Wadi Kid Core Complex. At stage A, shortening took place with subduction in an island-arc setting, and extensive crustal thickening (D_1). At stage B, convection at the root initiated extension. At C the actual collapse started with the formation of low-angle normal faults, including the detachment fault (D_{2a}). At stage D granitoids intruded, causing local reversal of the sense of shear due to upwarping of the detachment fault (D_{2b}). Stage E shows the situation as observed today (Figure 11) with the late Precambrian shear directions. Ages are interpreted from literature data (Table 4).

Table 4. Timing of the different phases of metamorphism and deformation in the Wadi Kid area as deduced from the literature (see 'Geological background').

Age	Deformation	Deformation features	Metamorphism (facies)
pre-620 Ma*	D_1	S_1, F_1 folds	M_1 (lower greenschist)
620–560 Ma*	D_2 (Main phase)	S_2, lineation, deformed elliptical objects, rotated clasts, e.c.c.'s, asymmetric folds, quartz c-axis fabrics	M_2 (upper greenschist to amphibolite)
post-560 Ma	D_2 (Shear sense reversal)	"	"

* In the literature (e.g. Bielski 1982, Halpern & Tristan 1981) some D_2 rocks were dated pre-620 Ma, whereas D_1 was also dated at pre-620 Ma. To the north, older ages were recorded for D_1. No dates are available for the low-grade rocks in the Wadi Kid area (e.g. the Beda Turbidites). These dates, interpreted by Bielski (1982) and Halpern & Tristan (1981) as D_1, may very well reflect D_2 ages. Mafic xenoliths resembling rocks of the Malhaq and Heib Fms were found in deformed diorites dated at 620 Ma and indicate that volcanism took place well before 620 Ma ago.

at LP/HT conditions occurred. These intrusions caused the uplift and flexure of the shear zone, and normal movement to the southeast started at their southeasterly sides. The SE movement, as recorded in some 30% of the shear indicators, is thus an overprint. This is in accordance with our metamorphic studies, which show that white micas are predominantly present in the SE-vergent shear-indicators. The SE movement was due to normal movement in a shear zone along the SE side of an intruding granite, northwest of the Wadi Kid area, at the later stages of the formation of the core complex. Ayalon et al. (1987) found evidence in amphibolite schists for a second thermal pulse at 560–530 Ma, after the main phase at 600 Ma. This phase can be related to the intrusion of younger plutons and so the shear reversal event can be dated at 560–530 Ma.

The general trend of the quartz c-axis fabrics shows a transition from a stronger coaxial component at the lower structural levels to a stronger non-coaxial component at higher structural levels. This is in agreement with findings of Malavieille (1993) for quartz c-axis studies of the core complexes in the Basin and Range province, U.S.A. He concluded that low-angle normal shear zones will show a strain distribution through such a shear zone as described above for the quartz c-axis fabrics, contrary to compressional settings, where a homogeneous distribution of strain is to be expected (Malavieille 1993). He attributes this variation in the style of deformation through extensional shear zones to the different amount of rotational strain between the highly deformed upper crustal rocks of the hanging wall and the less deformed basement in the footwall, below the shear zone. This also explains the coaxial component of strain, as observed in the deformed xenoliths within the gneissic lower-crustal diorites. Malevieille (1993) also demonstrated that deformation, in the shearzone, will be increasingly non-coaxial away from the axis of the dome. This all explains the complex strain patterns in the Wadi Kid area.

A model for the tectonic history of the Wadi Kid area

Our model for the tectonic development of the Wadi Kid area in the late Precambrian is summarized in Figure 12 and Table 4. In an island-arc setting, volcanics of the Heib and Tarr Fms were deposited prior to 620 Ma. In this period, compression caused by the subduction was responsible for the D_1 deformation phase. At the same time, or slightly afterwards, I-type granitoids intruded. After a phase of crustal thickening related to the subduction of an oceanic plate, orogenic collapse started with extension in NW-SE direction, starting at 620 Ma. The schistose units of the Malhaq, the Umm Zariq, and the northern and western Heib Fms, and the deformed tonalites and diorites testify to the low-angle shear zone. During the extensional phase, dyke swarms intruded with a NE-SW strike. All the units were intruded by granites. The main movement along the shear zone was to the northwest, as deduced from the indicators of finite strain. Doming of younger NE-SW trending granitoid bodies near the Wadi Kid area caused upwarping of the main shear zone and reversal of the sense of shear. The heterogeneous strain distribution through the shear zone was responsible for the coaxial component as observed in the deformed

xenoliths and the c-axis fabrics. Deformation continued until after intrusion of the late granites.

The core-complex model explains why the D_1 shortening phase is only found at the upper crustal levels, while the horizontal cleavage is observed at lower crustal levels.

Conclusions

The Precambrian rocks in the Wadi Kid area display two main phases of deformation: D_1 and D_2. The present study offers new data and interpretations and leads to the following conclusions:

1) D_1 is a compressional phase related to island-arc subduction as recorded from F_1 folds and the S_1 foliation. It took place before 620 Ma.
2) A D_2 deformation phase, dated at 620–580 Ma, was responsible for the main structural features in the area, i.e. the sub-horizontal foliation and the well-developed stretching lineation. The foliation was formed due to mylonitization in a low-angle normal shear zone. The mineralogy indicates that the deformation took place at LP/HT conditions.
3) Shear indicators and quartz c-axis fabrics confirm that non-coaxial deformation took place. Finite strain markers such as deformed xenoliths and pebbles indicate a movement of the top block to the northwest in the shear zones. Most of the shear indicators, such as rotated clasts with pressure shadows, extensional crenulation cleavage, and quartz c-axis fabrics also indicate NW-vergent shear, but some indicate movement to the southeast.
4) The reversal of movement along mylonites was caused by upwarping due to the intrusion of granitoid bodies near the Wadi Kid area at the latest stages of the Pan-African orogenesis, 560–530 Ma ago.
5) Dyke swarms, dated at 590–580 Ma, striking NE-SW and perpendicular to the lineation indicate extension in NW-SE direction.
6) The structures and metamorphism observed, support a core-complex model for the Wadi Kid area.
7) The transition from the D_1 compressional regime to the D_2 extensional regime was due to orogenic collapse.

Acknowledgements

This research was supported by the Dr. Schürmann Foundation for Precambrian Research, grant no. 1994/06. We thank Harry N.A. Priem who helped at all stages of this project and critically read the manuscript. We also thank him for making available previously unpublished geochronological data. We appreciate the help by Abdel Aziz Hussein, Ibrahim Shalaby and Mohammed Tulba, of the Egyptian Geological Survey and Mining Authority in Cairo, Egypt. We thank R. Greiling for reviewing the paper. The comments on the manuscript by Dick A.J. Batjes are highly appreciated.

References

Ahmed, A.M., Y.L. El Sheshtawi & M.M. El Tokhi 1993 Origin and geochemistry of Egyptian granitoid rocks in Nuweiba area, eastern Sinai – J. African Earth Sci. 17: 399–413

Anderson, J.L. & R.L. Cullers 1990 Middle to upper crustal plutonic construction of a magmatic arc; An example from the Whipple Mountains metamorphic core complex. In: J.L. Anderson (ed.) The Nature and Origin of Cordilleran Magmatism – Geol. Soc. Am. Mem. 174: 47–69

Ayalon, A., G. Steinitz & A. Starinsky 1987 K-Ar and Rb-Sr whole rock ages reset during Pan-African event in the Sinai Peninsula (Ataqa Area) – Precambrian Res. 37: 191–197

Barton, M.D. 1990 Cretaceous magmatism, metamorphism and metallogeny in the east-central Great Basin. In: J.L. Anderson (ed.) The Nature and Origin of Cordilleran Magmatism – Geol. Soc. Am. Mem. 174: 283–302

Bell, T.H. & R.L. Hammond 1984 On the internal geometry of mylonite zones – J. Geol. 92: 667–686

Bentor, Y.K. 1985 The crustal evolution of the Arabo-Nubian Massif with special reference to the Sinai Peninsula – Precambrian Res. 28: 1–74

Beyth, M., R.J. Stern, R. Altherr & A. Kröner 1994 The late Precambrian Timna igneous Complex, Southern Israel: Evidence for comagmatic-type sanukioid monzodiorite and alkali granite magma – Lithos 31: 103–124

Bielski, M. 1982 Stages in the Arabian-Nuvian Massif in Sinai (unpublished Ph.D. Thesis) – Hebrew University, Jerusalem, 155 pp

Choukroune, P., D. Gapais & O. Merle 1987 Shear criteria and structural symmetry – J. Struc. Geol. 9: 525–530

Cobbold, P.R. & D. Gapais 1987 Shear criteria in rocks: an introductory review – J. Struc. Geol. 9: 521–523

Davis, G.H. 1980 Structural characteristics of metamorphic core complexes, southern Arizona. In: M.D. Crittenden, P.J. Coney & G.H. Davis (eds.) Cordilleran Core Complexes – Geol. Soc. Am. Mem. 153: 35–77

Davis, G.A. & G.S. Lister 1988 Detachment faulting in continental extension; Perspectives from the Southwest U.S. Cordillera – Geol. Soc. Am. Spec. Paper 218: 133–159

Dewey, J.F. 1988 Extensional collapse of orogens – Tectonics 7: 1123–1139

Dunner, D. 1969 A technique of finite strain analysis using elliptical particles – Tectonophysics 7: 117–136

Eyal, E., M. Eyal & A. Kroner 1991 The geochronology of the Elat terrain, metamorphic basement, and its implication for crustal evolution of the NE part of the Arabian-Nubian Shield – Isr. J. Earth Sci. 40: 5–16

Folkman, Y. & R. Assael 1980a Gravity map of Sinai (relative Bouguer anomalies); 1:500 000 – Survey of Israel, Jerusalem

Folkman, Y. & R. Assael 1980b Aeromagnetic map of Sinai; 1:500 000 – Survey of Israel, Jerusalem

Fueten, F., P-Y.F. Robin & R. Stephens 1991 A model for the development of a dominal quartz c-axis fabric in a coarse-grained gneiss – J. Struc. Geol. 13: 1111–1124

Furnes, H., A.E. Shimron & D. Roberts 1985 Geochemistry of Pan-African volcanic arc sequences in southeastern Sinai Peninsula and plate tectonic implications – Precambrian Res. 29: 359–382

Gautier, P. & J.P. Brun 1994 Ductile crust and exhumation and extensional detachments in the central Aegean (Cyclades and Evvia Islands) – Geodinamica Acta 7: 57–85

Ghazala, H.H. 1995 Structural interpretation of the Bouguer and aeromagnetic anomalies in the central Sinai – J. African Earth Sci. 19: 35–42

Greiling, R.O., M.M. Abdeen, A.A. Dardir, H. El Akhal, M.F. El Ramly, G.M. Kmal El Din, A.F. Osman, A.A. Rashwan, A.A. Rice & M.F. Sadek 1994 A structural synthesis of the Proterozoic Arabian-Nubian Shield in Egypt – Geol. Rundschau 83: 484–501

Halpern, M. 1980 'Pan-African' isochron ages of Sinai igneous rocks – Geology 8: 639–648

Halpern, M. & N. Tristan 1981 Geochronology of the Arabian-Nubian Shield in southern Israel and eastern Sinai – J. Geol. 89: 639–648

Hanmer, S. 1986 Asymmetrical pull-aparts and foliation fish as kinematic indicators – J. Struc. Geol. 8: 111–112

Hazlett, R.W. 1990 Extension related Miocene volcanism in the Mopah Range volcanic field, southeastern California. In: J.L. Anderson (ed.) The Nature and Origin of Cordilleran Magmatism – Geol. Soc. Am. Mem. 174: 133–145

Husseini, M.I. 1988 The Arabian Infracambrian extensional system – Tectonophysics 148: 93–143

Jarrar, J., A. Baumann & H. Wachendorf 1983 Age determinations in the Precambrian basement of Wadi Araba area, southeast Jordan – Earth Planet Sci. Lett. 63: 292–304

Jessel, M.W. & G.S. Lister 1990 A simulation of temperature dependence of quartz fabrics. In: R.J. Knipe & E.H. Rutter (eds.) Deformation Mechanisms, Rheology and Tectonics – Geol. Soc. Spec. Public. 54: 335–352

Kohn, B.P. & M. Eyal 1981 History of the uplift of the crystalline basement of Sinai and its relation to the opening of the Red Sea as revealed by fission track dating of apatites – Earth Planet Sci. Lett. 52: 129–141

Law, R.D. 1990 Crystallographic fabrics: a selective review of their applications to research in structural geology. In: R.J. Knipe & E.H. Rutter (eds.) Deformation Mechanisms, Rheology and Tectonics – Geol. Doc. Spec. Publ. 54: 335–352

Le Theoff, B. 1979 Non-coaxial deformation of elliptical particles – Tectonophysics 53: T7–T13

Lisle, R.J. 1977 Estimation of the tectonic strain ratio from the mean shape of deformed elliptical markers – Tectonophysics 56: 140–144

Lisle, R.J. 1985 Geological Strain Analysis: A Manual for the R_f/Φ Technique. Pergamon, Oxford, 99 pp

Lister, G.S. & B.E. Hobbs 1980 The simulation of fabric development during plastic deformation and its application to quartzite: the influence of the deformation history – J. Struc. Geol. 2: 355–370

Lister, G.S., G. Banga & A. Feenstra 1984 Metamorphic core complexes of the Cordilleran type in the Cyclades, Aegean Sea, Greece – Geology 12: 221–225

Liu, M. & K.P. Furelong 1993 Crustal shortening and Eocene extension in the southeastern Canadian Cordillera: Some thermal and rheological considerations – Tectonics 12: 776–786

Malavieille, J. 1987 Kinematics of compressional and extensional ductile shearing deformation in a metamorphic core of the northern Basin and Range – J. Struc. Geol. 9: 541–554

Malavieille, J. 1993 Late orogenic extension in mountain belts: Insights from the Basin and Range and the Late Paleozoic Variscan Belt – Tectonics 12: 1115–1130

Means, W.D. 1994 Rotational quantities in homogeneous flow and the development of small scale structures – J. Struc. Geol. 16: 437–445

Platt, J.P. & R.L.M. Vissers 1980 Extensional structures in anisotropic rocks – J. Struc. Geol. 2: 397–410

Price, G.P. 1985 Preferred orientation in quartzites. In: H.R. Wenk (ed.): Preferred Orientation in Deformed Metals and Rocks. Academic Press, Orlando: 385–406

Price, N.J. & J.W. Cosgrove 1990 Analysis of geological structures. Cambridge University Press, 502 pp

Priem, H.N.A., M. Eyal, E.H. Hebeda & E.A.Th. Verdurmen 1984 U-Pb zircon dating in the Precambrian basement of the Arabo-Nubian Shield of the Sinai Peninsula – A progress report, ECOG VIII – Terra Cognita 4: 30–31

Ragab, A.I. 1993 A geodynamic model for the distribution of the oceanic plate slivers within a Pan-African orogenic belt, Eastern Desert, Egypt – J. Geodynamics 17: 21–26

Reymer, A.P.S. 1983 Metamorphism and tectonics of a Pan-African terrain in southeastern Sinai – Precambrian Res. 19: 225–238

Reymer, A.P.S. 1984 Metamorphism and tectonics of a Pan-African terrain in southeastern Sinai – A Reply – Precambrian Res. 24: 189–197

Reymer, A.P.S., A. Matthews & O. Navon 1984 Pressure-temperature conditions in the Wadi Kid metamorphic Complex: implications for the Pan-African event in SE Sinai – Contrib. Miner. Petrol. 85: 336–345

Reynolds, S.J. & G.S. Lister 1990 Folding of mylonitic zones in Cordilleran core complexes: Evidence from near the mylonitic front – Geology 18: 216–219

Schmid, S.M. & M. Casey 1986 Complete fabric analysis of some commonly observed quartz c-axis patterns – Am. Geophys. Union, Geophys. Monogr. 36: 263–286

Shackleton, R.M., A.C. Ries, R.H. Graham & W.R. Fitches 1980 Late Precambrian ophiolitic melange in the eastern desert of Egypt – Nature 285: 472–474

Shimron, A.E. 1980 Proterozoic island arc volcanism and sedimentation in Sinai – Precambrian Res. 12: 437–455

Shimron, A.E. 1983 The Tarr Complex revisited. The Tarr Complex: folding, thrusts and melanges in the southern Wadi Kid region, Sinai Peninsula – Isr. J. Earth Sci 32: 123–148

Shimron, A.E. 1984 Metamorphism and tectonics of a Pan-African terrain in southeastern Sinai – A discussion – Precambrian Res. 24: 173–188

Shimron, A.E. 1987 Pan-African metamorphism and deformation in the Wadi Kid region, SE Sinai Peninsula: evidence from porphyroblasts in the Umm Zariq Formation – Isr. J. Earth Sci. 36: 173–193

Siender, G., J.R. Pringle & A.E. Shimron 1974 Age of relationships in basement rocks of the Sinai Peninsula. Proc., Int. Meetings Geochronology, Cosmochronology and Isotope Geology, Paris

Simpson, C. & S.M. Schmid 1983 An evaluation of criteria to deduce the sense of movement in sheared rocks – Geol. Soc. Am. Bull. 94: 1281–1288

Spencer, J.E. 1984 Role of tectonic denudation in warping and uplift of low-angle normal faults – Geology 12: 95–98

Stern, R.J. 1985 The Najd fault system, Saudi Arabia and Egypt: A late Precambrian rift related transform system? – Tectonics 4: 497–511

Stern, R.J. & W.I. Manton 1987 Age of Feiran basement rocks, Sinai: implications for late Precambrian crustal evolution in the northern Arabian-Nubian Shield – J. Geol. Soc. 144: 569–575

Ten Brink, C.E. 1996 Development of porphyroclast geometries during non-coaxial flow: An experimental and analytical investigation. Geol. Ultraiectina 142, 163 pp

Tullis, J., J.M. Christie & D.T. Griggs 1973 Microstructures and preferred orientations of experimentally deformed quartzites – Geol. Soc. Am. Bull. 84: 297–314

Twiss, R.J. & E.M. Moores 1992 Structural Geology. Freeman, 532 pp

Vail, J.R. 1985 Pan-African (Late Precambrian) tectonic terrains and the reconstruction of the Arabian-Nubian Shield – Geology 13: 839–842

Wernicke, B. 1985 Uniform-sense normal simple shear of the continental lithosphere – Can. J. Earth Sci. 22: 108–125

Worthing, M.A. 1984 Rotated boudins associated with Caledonian thrusting from Seiland, North Norway – Norsk Geol. Tidsskrift 64: 275–285